


Dry Active Matter Exhibits a Self-Organized Cross Sea Phase

Rüdiger Kürsten[✉] and Thomas Ihle

Institut für Physik, Universität Greifswald, Felix-Hausdorff-Straße 6, 17489 Greifswald, Germany

 (Received 15 February 2020; revised 3 August 2020; accepted 6 October 2020; published 30 October 2020)

The Vicsek model of self-propelled particles is known in three different phases: a polar ordered homogeneous phase, also called the Toner-Tu phase, a phase of polar ordered regularly arranged high density bands with surrounding low density regions without polar order, and a homogeneous phase without polar order. Here, we show that the standard Vicsek model has a fourth phase for large system sizes: a polar ordered cross sea phase. We demonstrate that the cross sea phase is not just a superposition of two waves, but it is an independent complex pattern with an inherently selected crossing angle.

DOI: [10.1103/PhysRevLett.125.188003](https://doi.org/10.1103/PhysRevLett.125.188003)

Active matter is characterized by the transformation of free energy into motion. The energy is supplied, e.g., by chemicals, external fields, or radiation. On the other hand, active particles dissipate energy into their environment such that there is an interplay between energy supply and dissipation.

Active entities appear from microscopic length scales or even below, e.g., for bacteria, Janus particles or molecular motors up to macroscopic sizes such as for birds, fish, mammals, or robots. They might be living organisms or artificially manufactured nonliving objects. Several reviews give an overview of the field [1–5]. Theoretical descriptions involve field or kinetic theories, see, e.g., [6–13].

Usually, active particles are surrounded by a fluid such as water or air. In many cases, the fluid is important, in particular, due to the conservation of momentum. Examples are swimming bacteria or artificial microswimmers that have been subject to intense research over the last decades, see, e.g., [14–16] for some reviews.

However, there is also a large class of active systems where the fluid can be neglected, e.g., particles moving close to a surface which can transfer arbitrary amounts of momentum to the environment, and thus, momentum conservation is effectively not an issue. Such systems with negligible fluid are called dry [1] and can be modeled by stochastic equations including positive and negative (activity) dissipation [3]. An important limiting case of strong activation and dissipation leads to a constant particle speed, an ingredient that is often directly incorporated in simplified models. One such model was introduced 25 years ago by Vicsek *et al.* [17] and is still one of the simplest and most studied models of active matter today. In the two-dimensional Vicsek model, one considers N point particles at positions \mathbf{r}_i that move with constant speed v in individual directions given by angles ϕ_i

$$\dot{\mathbf{r}}_i(t) = v \begin{pmatrix} \cos \phi_i(t) \\ \sin \phi_i(t) \end{pmatrix}, \quad (1)$$

where $i \in \{1, \dots, N\}$ is the particle index. The directions ϕ_i change at discrete instances of time $n\Delta t$, $n \in \mathbb{N}$ and remain constant between those collisions. These interactions are given by the following rule:

$$\phi_i(t + \Delta t) = \Theta \left[\sum_{j \in \Omega_i(t + \Delta t)} \begin{pmatrix} \cos \phi_j(t) \\ \sin \phi_j(t) \end{pmatrix} \right] + \xi_i(t), \quad (2)$$

where the set Ω_i contains the indexes of all particles j that satisfy $|\mathbf{r}_i - \mathbf{r}_j| < R$ for some interaction radius R . The function $\Theta(\mathbf{v})$ returns the angle that describes the direction of the two dimensional vector \mathbf{v} . The $\xi_i(t)$ are independent random variables drawn uniformly from the interval $[-\pi\eta, \pi\eta]$ with noise strength $\eta \in [0, 1]$. That is, after a discrete time interval Δt , all particles reorient due to interactions. The model exhibits a transition towards collective motion for small noise (or large density) that was first believed to be continuous [17]. This shows the nonequilibrium nature of active matter, since in equilibrium such a transition would be strictly forbidden for short-range interactions in two dimensions [18,19]. It was found later that, for large enough systems, the transition is actually discontinuous and goes along with the formation of high density bands that arrange regularly into waves [20–22]. For even smaller noise strength (or higher density), there is another transition towards (on large scales) a homogeneous polar ordered phase that is also called the Toner-Tu phase [21,23]. The behavior of the model has been described in analogy to a liquid-gas transition [23,24]. The disordered phase at high noise intensities is considered as a gas, see Fig. 1(iv) for a snapshot of this phase. The phase of polar ordered bands is considered as the coexistence of a polar ordered liquid (the bands) and a disordered gas (the particles between the bands with almost no polar order), see Fig. 1(iii) and the Toner-Tu phase is considered as a pure polar ordered liquid, see Fig. 1(i). It was observed in phase (iii), but close to phase (i), that the bands do not

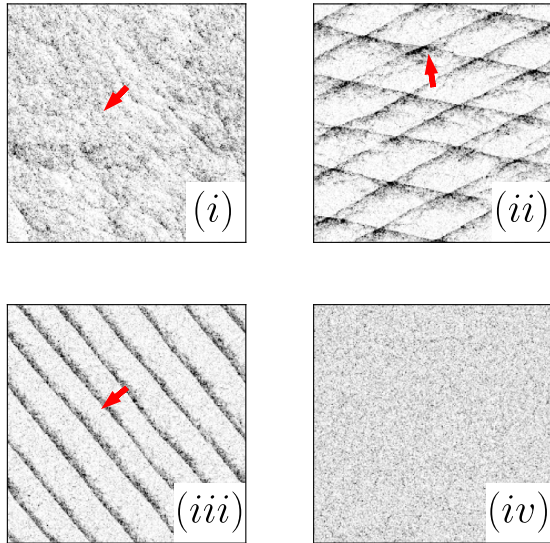


FIG. 1. Snapshots of the two dimensional standard Vicsek model in its four phases: (i) Toner-Tu phase also called polar ordered liquid ($\eta = 0.22$). (ii) Cross sea phase ($\eta = 0.30$). (iii) Band phase ($\eta = 0.37$). (iv) Disordered phase ($\eta = 0.45$). Dark color represents high particle density. Red arrows indicate the average direction of motion. Simulations have been started at random initial conditions. The snapshots have been taken after a thermalization time of $T = 2 \times 10^5$. System parameters: $R = 1$, $v = 1$, $\Delta t = 1$, particle number $N = 10^6$, system size $L = 1253.3$. On average, there are two particles within a unit circle. Periodic boundary conditions have been used.

achieve a smectic arrangement, but that they interact strongly and do not order, see Fig. 2(b) of Ref. [1]. It was explicitly formulated as a pending issue in [1] whether this state should be considered separately from phase (iii).

In this Letter, we answer this question by demonstrating that the aforementioned state represents another fourth phase of the Vicsek model that has not been reported before to the best of the authors' knowledge. In Fig. 1(ii), we show a snapshot of this fourth phase which looks like a cross sea. This phenomenon is sometimes observed in oceans when two wave systems like a swell (waves that are no longer under wind influence) and a wind sea (waves generated by wind) are combined, see, e.g., [25]. It is believed to be particularly dangerous for ships, see, e.g., [26]. Here, however, this cross sea pattern is self-organized, as there is no external driving. Crossing bands have been reported in different models before [27,28]. We demonstrate below that the cross sea pattern of the Vicsek model is not just a superposition of two planar waves. Instead, we find that the particle density at the crossing points of the pattern is much higher than the sum of two bands. Furthermore, the crossing angle is inherently selected.

We performed simulations for $N = 10^6$ particles in a quadratic domain of size $L = 1253.3$ with periodic boundary conditions. Other system parameters are $R = \Delta t = v = 1$, and the noise strength was varied from

$\eta = 0.2$ to $\eta = 0.49$ in steps of 0.01 simulating 15 realizations [29] for each noise. We made snapshots after $T = 2 \times 10^5$ thermalization time steps [30]. For the smallest noise strengths $\eta = 0.20, \dots, 0.24$, we observe more or less homogeneous states. Starting from about $\eta = 0.25$, structures are formed, and for $\eta = 0.27$, the first cross sea state arises. For $\eta = 0.29, 0.30$, all observed realizations are in a cross sea state. Starting from $\eta = 0.31$, some of the realizations are clearly cross sea, and some others are clearly bands, whereas for $\eta = 0.43, 0.44$, there are only band state realizations. Eventually, for $\eta \geq 0.45$, all realizations are disordered, see Supplemental Material [31]. Hence, we observe three transitions between four different phases.

To study the transitions in greater detail, we investigate a correlation order parameter that was recently introduced in [32] and suggested to be used in the study of structural phase transitions, in particular, out of equilibrium. It is a local integral over the two particle correlation function formally given by

$$C_2 := N^2 \int_{\mathbb{R}^2} G_2(\mathbf{r}_1, \mathbf{r}_2) d\mathbf{r}_1 d\mathbf{r}_2 \theta(R - |\mathbf{r}_1|) \theta(R - |\mathbf{r}_2|), \quad (3)$$

where $G_2(\mathbf{r}_1, \mathbf{r}_2) := P_2(\mathbf{r}_1, \mathbf{r}_2) - P_1(\mathbf{r}_1)P_1(\mathbf{r}_2)$ for one- and two-particle probability density functions P_1 and P_2 , θ is the Heaviside function. For isotropic systems, the parameter can be expressed in terms of the usual pair correlation function $g(r)$ as

$$C_2 = \left(\frac{N}{L^2}\right)^2 \int_{\mathbb{R}^2} [g(|\mathbf{r}_2 - \mathbf{r}_1|) - 1] \times \theta(R - |\mathbf{r}_1|) \theta(R - |\mathbf{r}_2|) d\mathbf{r}_1 d\mathbf{r}_2. \quad (4)$$

It is zero for independent particles and large when particles cluster together. Usually, it changes strongly when drastic spatial rearrangements occur. Thus, it is appropriate to study the phase transition that we observe here.

In Fig. 2, we show the average over 15 realizations [29] and 10^4 time steps of the C_2 order parameter in dependence on the noise strength. It clearly increases at the transition from phase (i) to phase (ii), then, it decreases from phase (ii) to phase (iii) and decreases much more at the transition from phase (iii) to phase (iv). In the average over all realizations (solid blue line), we cannot detect the transition between phases (ii) and (iii) that clearly, because for a relatively large noise range, we find realizations in both states, as discussed above. However, if we measure the order parameter for realizations that show bands or cross sea states separately, we find significant differences in C_2 , see red and green lines in Fig. 2. The clear separation of the two lines shows the discontinuous nature of the transition, which is also expected due to the different symmetry properties of the patterns. The observation that, at noise values where both patterns can coexist, the dominant

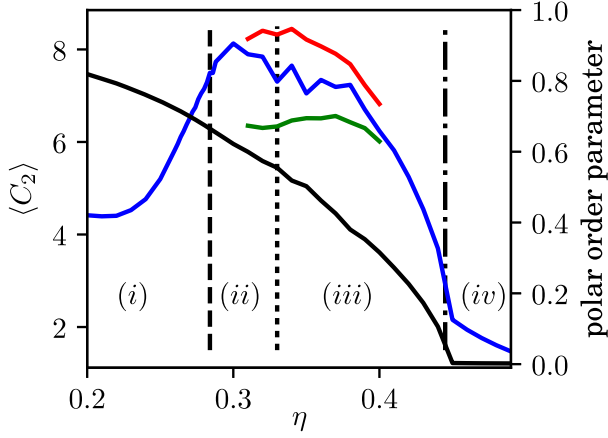


FIG. 2. Structural order parameter C_2 (blue line) and polar order parameter $p = 1/N |\sum_i \mathbf{v}_i|$ (black line) averaged over 15 realizations [29] and 10^4 time steps after a thermalization time of $T = 2 \times 10^5$ [30] (blue solid line). For the noise values $\eta = 0.31, \dots, 0.40$ we find several realizations in the cross sea phase as well as in the band phase, see Supplemental Material [31]. Averaging only over realizations that are identified (by hand) as clearly in the cross sea phase, results in the red upper line. Analogously, averaging over the band phase realizations only, results in the green lower line. We see that the correlation parameter C_2 increases from the Toner-Tu phase (i) to the cross sea phase (ii) and then decreases to the band phase (iii) and even more to the disordered phase (iv). The transition lines from (i) to (ii) and (ii) to (iii) (vertical dashed and dotted lines) have been obtained as dips of the Binder cumulant, see Fig. 3. The transition towards disorder (dash-dotted vertical line) was obtained by hand as all realizations are bands for $\eta = 0.44$ and all realizations are disordered for $\eta = 0.45$, see Supplemental Material [31]. Parameters are as in Fig. 1.

wavelength of the cross sea pattern is about twice as large as the one of the band pattern, see [31], provides further evidence for the discontinuous nature of the transition.

In order to justify whether the cross sea state is really a different phase, we measure the Binder cumulant of the C_2 order parameter that is defined as $1 - \langle C_2^4 \rangle / (3 \langle C_2^2 \rangle^2)$. In Fig. 3, we see that there are two dips separating phases (i) and (ii), and (ii) and (iii), respectively. In principle, we expect a third dip indicating the transition from phases (iii) to (iv). However, it has been shown in [32] that this dip is extremely sharp for large system sizes and, thus, not covered by the resolution of noise strength used here. Instead, we identify the position of the transition $\eta_{c3} \approx 0.445$ by direct visual inspection of the snapshots. The other transition noise strengths obtained from the dips in the Binder cumulant, $\eta_{c1} = 0.284$ and $\eta_{c2} = 0.33$, are also consistent with the phases identified on the snapshots. The minimum value of the Binder cumulant at a discontinuous transition depends on the distribution of the order parameter. For large systems, it depends in leading order only on the positions of the two peaks of the distribution, see [33]. For the transition between (ii) and (iii), we can

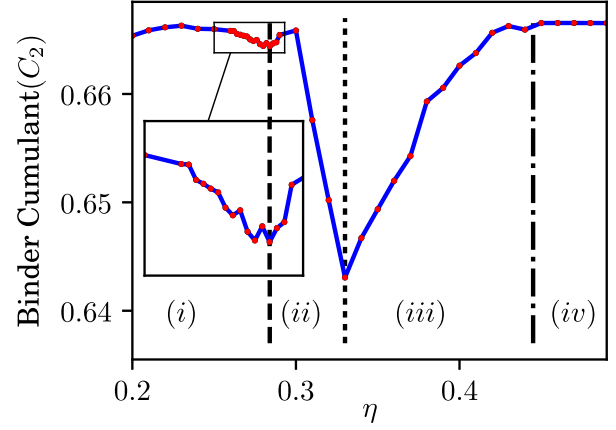


FIG. 3. Binder cumulant of the structural order parameter C_2 obtained from the same simulations as used in Fig. 2. We can identify two clear dips indicating the transitions from phases (i) to (ii) (dashed line) and from phases (ii) to (iii) (dotted line). In the inset, we show some additional points [29] close to the transition from phase (i) to (ii). In principle, there should be a third dip between phases (iii) and (iv) (dash-dotted line). However, this is not observed here due to its expected sharpness.

estimate those peak positions by the averages of cross sea and band states, that is, by the red and the green line of Fig. 2. According to the theory of [33], we obtain a minimum value of the Binder cumulant that deviates only about 0.3% from the measured value. For the transition between (i) and (ii), we directly measure the distribution of the order parameter, obtaining a double peak distribution. The minimum value of the Binder cumulant predicted from those peak positions also agrees with the measured value within the estimated uncertainty, see, for details, [31]. Thus, the fact that the dip in the Binder cumulant at η_{c1} is relatively small does not indicate that there is no real transition. In contrast, the size of the dip is in accordance with the theory of first order transitions [33]. We also study different system parameters and find qualitatively equivalent results, see [31].

Looking at Fig. 1(ii), we might suppose that the cross sea state is just a superposition of two planar waves as they occur in phase (iii). To test this hypothesis, we measure the particle density averaged in the comoving frame [34] of the cross sea pattern. One example is displayed in Fig. 4(a). We observe that the density at the crossing points of the pattern is much larger than the sum of the densities of two fronts. This shows that the cross sea state represents a stand-alone complex pattern and not just the superposition of two waves, such as, e.g., in [27]. Even more evidence for the independence of the pattern is obtained from the distribution of crossing angles. For a superposition of waves, all crossing angles would be allowed. However, we find only one inherently selected crossing angle, see Supplemental Material [31].

Considering only the high density crossing points of the pattern, the system looks like a two-dimensional lattice of

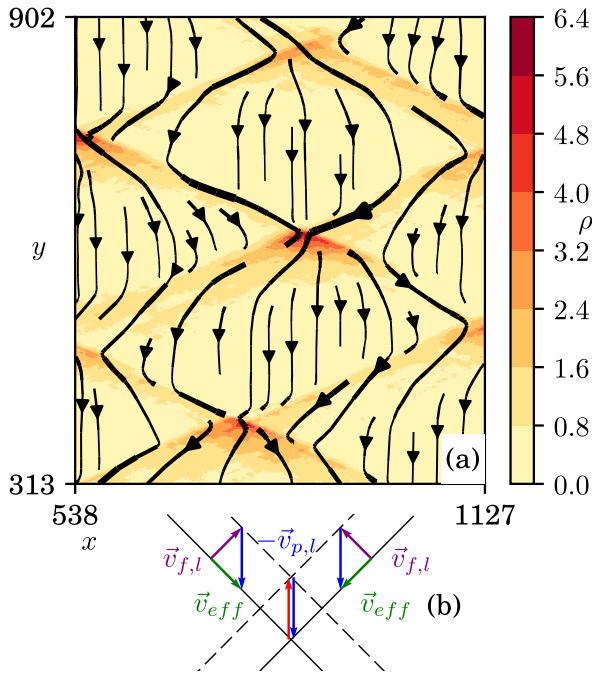


FIG. 4. (a) Average of local particle density ρ and local momentum density over 10^3 time steps after a thermalization time of $T = 2 \times 10^5$ within the comoving frame [35] of the cross sea pattern. The particle density is displayed by the color map. One sees that a lot of mass accumulates at the crossing points of the pattern. The densities of the crossing points are approximately four to five times as large as the density along the single fronts. The black arrows display the momentum density, where thick arrows correspond to large momentum. We see that mass is mainly transported along the high density bands and, on average, in the opposite directions of the mean velocity of the particles in the lab frame (red arrow). Parameters are as in Fig. 1, $\eta = 0.29$. (b) Illustration of the mass transport mechanism within the pattern. See text for explanations.

particle clusters. Such a lattice was found in a Vicsek-like model with additional repulsive interactions and special boundary conditions [35]. Here, however, the fronts connecting the clusters cannot be neglected because they are necessary to transmit information between the crossing points. But it is still reasonable to investigate a lattice order parameter. Qualitatively, such an order parameter looks exactly like the structural order parameter C_2 of Fig. 2 and, thus, confirms the presence of the cross sea phase, see [31] for details.

To understand the accumulation of mass at the crossing points of the pattern, we also investigate the momentum density within the comoving reference frame [34] of the pattern. We observe a nonzero particle flow along the band structures of the pattern, on average, in the direction opposite to the movement of the pattern in the lab frame, see Fig. 4(a). This shows that, in the lab frame, the pattern moves faster than the center of mass. In the example of Fig. 4(a) the pattern velocity is $|\vec{v}_{p,l}| \approx 0.92$ compared to

the center of mass velocity $|\vec{v}_{cm,1}| \approx 0.65$. Qualitatively, the particle flow can be understood by a simple geometric argument, shown in Fig. 4(b). In the lab frame, the particles in the band move, on average, perpendicular to the fronts with velocity $\vec{v}_{f,l}$. However, the whole pattern moves with velocity $\vec{v}_{p,l}$ in the lab frame. Considering the band particles in the pattern comoving frame [34], their velocity is given by $\vec{v}_{eff} = \vec{v}_{f,l} - \vec{v}_{p,l}$ which points along the front, see Fig. 4(b). At the crossing points, however, the particle velocities point, on average, in the same direction as the pattern velocity [indicated by the red arrow in Fig. 4(b)]. Because of the high local density, there is stronger alignment at the crossing points, such that the mean local velocity can reach the pattern velocity $\vec{v}_{p,l}$. This mechanism transports mass along the bands towards the crossing points. In steady state, it is compensated by mass loss due to not perfectly ordered particles that lose contact to the crossing points and enter the low density region behind the bands.

In summary, in this numerical study, we have shown that the two-dimensional standard Vicsek model forms complex self-organized cross sea patterns for very large system sizes and in certain parameter regimes. We measured the density profile of the pattern and found that it is not just a superposition of two waves but an independent structure. We observe an interesting mass transport in the opposite direction compared to the pattern propagation leading to particle accumulation at the crossing points of the pattern. Furthermore, measuring the Binder cumulant of a correlation order parameter, we have shown that the cross sea pattern represents a fourth phase of the Vicsek model. There are two discontinuous transitions from the cross sea phase: for lower noise intensity, the system enters the Toner-Tu phase, and for higher noise intensity, it enters the phase of high density waves. Thus, we answer a recently formulated question [1]. On the other hand, a theoretical understanding of this novel phase is still missing. Natural candidates for mathematical descriptions are field or kinetic theories. Both approaches seem to be challenging, because a full two-dimensional treatment is likely to be necessary in contrast to the band phase. The appearance of the cross sea phase might also be relevant for other active matter models. However, further studies are required. Another pending question is whether an analogous phase exists in the three-dimensional Vicsek model. A remarkable result from the general view on active matter is that apparently single species active systems can form complex patterns similar to those known from reaction-diffusion systems.

The authors gratefully acknowledge the Gemeinsame Wissenschaftskonferenz support for funding this project by providing computing time through the Center for Information Services and High Performance Computing at TU Dresden on the HRSK-II. The authors gratefully acknowledge the Universitätsrechenzentrum Greifswald for providing computing time.

- [1] H. Chaté, *Annu. Rev. Condens. Matter Phys.* **11**, 189 (2020).
- [2] T. Vicsek and A. Zafeiris, *Phys. Rep.* **517**, 71 (2012).
- [3] P. Romanczuk, M. Bär, W. Ebeling, B. Lindner, and L. Schimansky-Geier, *Eur. Phys. J. Spec. Top.* **202**, 1 (2012).
- [4] S. Ramaswamy, *Annu. Rev. Condens. Matter Phys.* **1**, 323 (2010).
- [5] J. Toner, Y. Tu, and S. Ramaswamy, *Ann. Phys. (Amsterdam)* **318**, 170 (2005).
- [6] J. Toner and Y. Tu, *Phys. Rev. Lett.* **75**, 4326 (1995).
- [7] J. Toner and Y. Tu, *Phys. Rev. E* **58**, 4828 (1998).
- [8] E. Bertin, M. Droz, and G. Grégoire, *Phys. Rev. E* **74**, 022101 (2006).
- [9] E. Bertin, M. Droz, and G. Grégoire, *J. Phys. A* **42**, 445001 (2009).
- [10] J. Toner, *Phys. Rev. E* **86**, 031918 (2012).
- [11] T. Ihle, *Phys. Rev. E* **83**, 030901(R) (2011).
- [12] T. Ihle, *J. Stat. Mech.* (2016) 083205.
- [13] A. Nikoubashman and T. Ihle, *Phys. Rev. E* **100**, 042603 (2019).
- [14] M. Bär, R. Großmann, S. Heidenreich, and F. Peruani, *Annu. Rev. Condens. Matter Phys.* **11**, 441 (2020).
- [15] C. Bechinger, R. Di Leonardo, H. Löwen, C. Reichhardt, G. Volpe, and G. Volpe, *Rev. Mod. Phys.* **88**, 045006 (2016).
- [16] J. Elgeti, R. G. Winkler, and G. Gompper, *Rep. Prog. Phys.* **78**, 056601 (2015).
- [17] T. Vicsek, A. Czirók, E. Ben-Jacob, I. Cohen, and O. Shochet, *Phys. Rev. Lett.* **75**, 1226 (1995).
- [18] N. D. Mermin and H. Wagner, *Phys. Rev. Lett.* **17**, 1133 (1966).
- [19] P. C. Hohenberg, *Phys. Rev.* **158**, 383 (1967).
- [20] G. Grégoire and H. Chaté, *Phys. Rev. Lett.* **92**, 025702 (2004).
- [21] H. Chaté, F. Ginelli, G. Grégoire, and F. Raynaud, *Phys. Rev. E* **77**, 046113 (2008).
- [22] T. Ihle, *Phys. Rev. E* **88**, 040303(R) (2013).
- [23] A. P. Solon, H. Chaté, and J. Tailleur, *Phys. Rev. Lett.* **114**, 068101 (2015).
- [24] A. P. Solon, J.-B. Caussin, D. Bartolo, H. Chaté, and J. Tailleur, *Phys. Rev. E* **92**, 062111 (2015).
- [25] M. Onorato, D. Proment, and A. Toffoli, *Eur. Phys. J. Spec. Top.* **185**, 45 (2010).
- [26] A. Toffoli, J. Lefevre, E. Bitner-Gregersen, and J. Monbaliu, *Appl. Ocean Res.* **27**, 281 (2005).
- [27] A. M. Menzel, *Phys. Rev. E* **85**, 021912 (2012).
- [28] B. Bhattacharjee and S. Manna, *Physica (Amsterdam)* **531A**, 121733 (2019).
- [29] We used 100 realizations for the noise strengths $\eta = 0.25, 0.26, 0.262, 0.264, 0.266, 0.268, 0.27, 0.272, 0.274, 0.276, 0.278, 0.28, 0.282, 0.284, 0.286, 0.288, 0.29$, and 15 realizations for all other noise strength in the range $[0.20, 0.49]$ in steps of 0.01.
- [30] For the smallest noise strength in the disordered phase, $\eta = 0.45$, we still used $T = 2 \times 10^5$, for larger noise strengths, $\eta = 0.46, \dots, 0.49$, we used a shorter time of $T = 10^4$ because thermalization is much faster in the disordered phase.
- [31] See Supplemental Material at <http://link.aps.org/supplemental/10.1103/PhysRevLett.125.188003> for the analysis of a lattice order parameter, wave lengths and crossing angles of the pattern, estimates of relaxation times, and data and snapshots for additional parameter sets (different system sizes, densities, aspect ratios of the simulation box).
- [32] R. Kürsten, S. Stroteich, M. Z. Hernández, and T. Ihle, *Phys. Rev. Lett.* **124**, 088002 (2020).
- [33] J. Lee and J. M. Kosterlitz, *Phys. Rev. B* **43**, 3265 (1991).
- [34] The comoving frame of the patterns is defined as the Galilean reference frame in which the pattern (i.e., the particle density) does not move. To obtain it, we calculated, at each time step, a histogram of all positions of the particles before streaming. We then shifted the particle positions after streaming along the axis given by the mean velocity of all particles (among distances not greater than the particle speed v) and also made a histogram of the shifted after-streaming particle positions. We looked for the correlation between the histograms before streaming and after streaming with shift. The shift leading to the maximal correlation was then applied to all particles.
- [35] A. M. Menzel, *J. Phys. Condens. Matter* **25**, 505103 (2013).